Pure appl. geophys. 164 (2007) 547–564
0033–4553/07/030547–18
DOI 10.1007/s00024-006-0166-3

Pure and Applied Geophysics

Estimation of Tsunami Hazard in New Zealand due to South American Earthquakes

William Power, Gaye Downes, and Mark Stirling

Abstract—We develop a probabilistic model for estimating the tsunami hazard along the coast of New Zealand due to plate-interface earthquakes along the South American subduction zone. To do this we develop statistical and physical models for several stages in the process of tsunami generation and propagation, and develop a method for combining these models to produce hazard estimates using a Monte-Carlo technique. This process is largely analogous to that used for seismic hazard modelling, but is distinguished from it by the use of a physical model to represent the tsunami propagation, as opposed to the use of empirical attenuation models for probabilistic seismic hazard analysis.

Key words: Tsunami, New Zealand, probabilistic, hazard model, Monte Carlo.

Introduction

The location of New Zealand on the Pacific rim exposes it to a high risk of tsunami generated by great earthquakes located along the numerous subduction zones around the Pacific rim. This includes the Hikurangi-Kermadec subduction zone off the east coast of the North Island of New Zealand, and the Fiordland and Puysegur subduction zones in the southwest of the country. Tsunamis may also be locally generated by volcanoes or landslides on the continental shelf. However, for the initial development of the methodology of our probabilistic tsunami hazard analysis (PTHA) model we consider only distant source events; specifically those generated by South American earthquakes. Historically, these have been the most frequently occurring distant source of damaging tsunami in New Zealand, and therefore provide data against which to check the accuracy of the PTHA models. Three such tsunamis have had a significant, widely distributed and damaging impact along the east coast of New Zealand and on the offshore Chatham Islands (1000 km east of the main islands of New Zealand) in the last 150 years.

Probabilistic seismic hazard analysis (PSHA: Cornell, 1968; McGuire, 2004) is a well-established technique, of great value for developing appropriate hazard

GNS Science, 1 Fairway Drive, Avalon, PO Box 30368, Lower Hutt, New Zealand.

mitigation strategies. It is frequently used to determine the structural design specifications needed to withstand a specified return period ground-shaking, and indeed to determine whether a site is suitable for a particular application (e.g., a nuclear power plant). The destructive power of tsunamis so graphically demonstrated by the Sumatra tsunami of 26 December 2004 (BORRERO, 2005; GHOBARAH *et al.*, 2006), has drawn attention to the desirability of being able to apply similar probabilistic techniques to estimate tsunami hazard and so recognise the potential for events not experienced historically.

Until recently tsunami hazard has been regarded as very difficult to estimate in a probabilistic manner with sufficient accuracy to be of practical benefit. This is in large part due to the diversity and complexity of tsunami sources and the complexity of source-site propagation, which for the most part does not allow simple empirically derived attenuation relationships such as are used in seismic hazard analysis (for example, relationships describing the dependence of ground motions on distance from an earthquake source, and parameters of the earthquake such as magnitude and source mechanism) to be used without large uncertainties. Numerical models of tsunami propagation provide a means to approach the problem of PTHA by directly calculating the source-to-site relationship. RIKITAKE and AIDA (1988) estimated tsunami hazard probability for the east coast of Japan using numerical models of tsunamis originating from characteristic earthquake sources off the Pacific Coast of the Japanese Islands. ANNAKA *et al.* (2004; this issue) used a logic tree approach to estimate tsunami hazard at specific locations along the Japanese coast, incorporating a mixture of numerically modelled tsunami from local and distant earthquake sources. THIO *et al.* (2005; this issue) have estimated tsunami hazard in the Indian Ocean due to earthquakes off the coast of Sumatra, using an approach that allows for non-uniform slip on the earthquake rupture surface.

In this paper we present a new methodology for PTHA, which we illustrate with reference to the impact in New Zealand of tsunami from a particular group of tsunami sources, but which we believe can be extended to all distant and local earthquakes. Extension of the method to cover landslide sources is likely to be challenging, one key reason being that, in general, suitable magnitude/frequency relations for underwater landslides are difficult to establish. Volcanic and bolide sources can in principle be included, provided suitable physical models of tsunami initiation are available.

The methodology we describe is based on the use of Monte-Carlo simulations; MUSSON (2000) has made a comparison of conventional PSHA (as described in CORNELL, 1968; MCGUIRE, 2004) and the Monte-Carlo method of seismic hazard analysis, and his study of the relative pros and cons of each technique is equally applicable to tsunami hazard analysis. Monte-Carlo techniques have previously been used to study landslide tsunami hazard off Southern California (WATTS, 2004), and to evaluate the tsunami risk to New Zealand cities from local and distant earthquakes using empirical attenuation relationships (BERRYMAN, 2005).

Historical Background

The written historical record of tsunami in New Zealand covers less than two centuries, which is short compared to many similar countries bordering the Pacific, such as Japan (1500 years: IIDA *et al.*, 1967) and the South American states (500 years: LOCKRIDGE, 1985). Consequently events with long recurrence intervals will not be fully represented. Further, the historical record is likely to be incomplete (missing events, or missing data on known events) even over the time it spans due to the sparse population distribution in the early days of European settlement and due to the inhospitable nature of some regions (POWER *et al.*, 2005).

The historical record is supplemented by investigating tsunami recorded in the oral history of New Zealand's indigenous population, the Māori, and in the geological record. There are a number of events that could be interpreted as tsunami in Māori history and legends (MCFADGEN, pers. comm.), many of which were documented by early European missionaries, but it is difficult to attach specific dates to these events and to establish whether or not particular stories relate to the same event. Paleo-tsunami studies (for example, COCHRAN *et al.*, 2005; GOFF *et al.*, 2000; NICHOL *et al.*, 2003) have identified a number of large tsunami inundation events in the pre-historical period, but their sources are not always clear. What is clear is that New Zealand has a significant tsunami hazard problem that the shortness of the historical record may not adequately represent.

Nevertheless, the historical record indicates the important contribution of trans-Pacific tsunamis to New Zealand's tsunami hazard and risk, and the importance of fully understanding the tsunami risk from distant sources. For example, three well-documented historical trans-Pacific tsunami caused significant and widespread damage throughout the east coast of New Zealand. These were generated by the 1868 M_w 9.1 southern Peru, 1877 M_w 9.0 northern Chile, and 1960 M_w 9.5 southern Chile earthquakes, respectively (magnitudes from ITDB/PAC, 2004); details of these events are described in Appendix 1. Some very minor damage was caused by the tsunami generated by the 1946 M_w 7.9 Aleutian earthquake (OKAL *et al.*, 2002).

Not all events that caused damaging tsunami to propagate around the Pacific affected New Zealand. Only minor impact in New Zealand was experienced from tsunamis caused by the 1933 M_w 8.6 Japan, 1952 M_w 9.0 Kuril, 1957 M_w 8.7 Aleutian, 1964 M_w 9.5 Alaska, 1906 M_w 8.7 Columbia-Ecuador and the 1919 M_w 8.4 Tonga trench earthquakes (Fig. 1, magnitudes from ITDB/PAC, 2004). This is not unexpected given the orientation of these subduction zones and the large-scale radiation pattern for earthquake-generated tsunami that can be estimated using the techniques of BEN-MENAHEM and ROSENMAN (1972) (for a more recent perspective on this approach see OKAL (2003)). However bathymetric features can also have a significant impact on the propagation and affect the directivity in the

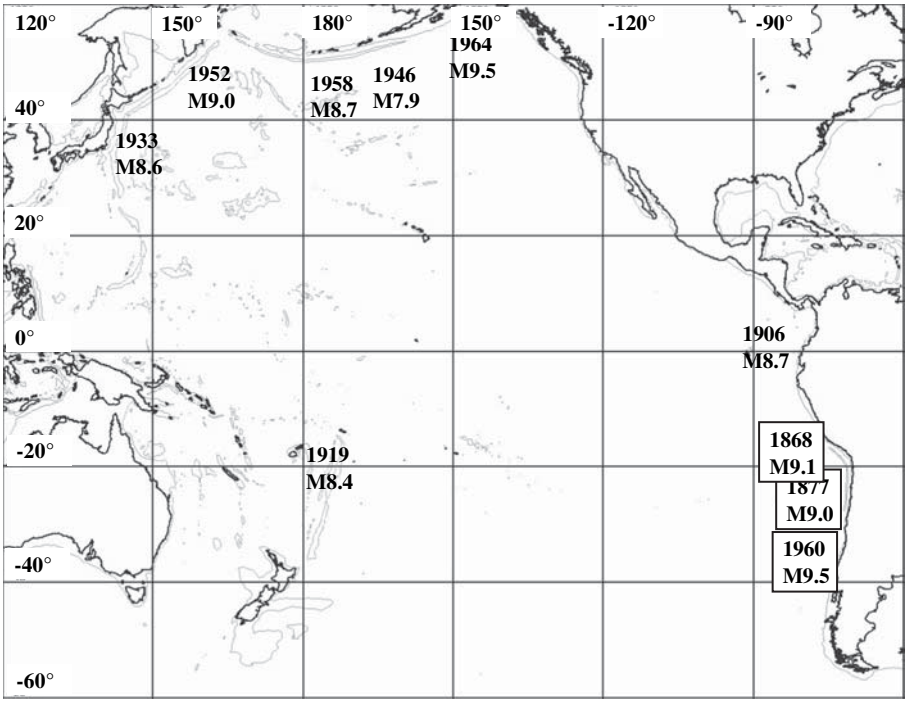

Figure 1
Locations of selected great earthquakes around the Pacific, boxes indicate that the earthquake had a significant impact on New Zealand. Magnitudes and outline map from Integrated Tsunami Database for the Pacific (ITDB/PAC, 2004).

far-field, as was apparent following the 2004 Sumatra tsunami (TITOV *et al.*, 2005). For this reason, the possibility of damage being caused by larger tsunamis originating from less-than-optimally oriented regions cannot be excluded without some investigation using numerical models. This is particularly important for areas which have not been the source of great earthquakes in the last 200 years, such as Central America, Cascadia, the Kermadec trench and the Southern Ocean.

Investigation of the magnitude/frequency distribution of large subduction zone earthquakes, numerical modelling of tsunami and the development of PTHA has the potential to identify the level of threat that goes beyond the historical record, and allows estimation of the hazard in terms of return periods commonly used for analysis of natural hazards, such as 100, 500, and 2,500 years. As with PSHA, the historical and pre-historical records are useful for validating the source-to-site relationships (tsunami propagation models in PTHA, attenuation relations in PSHA), and for checking the reliability of the hazard estimates.

Methodology

In principle there is the potential for many different tsunamigenic earthquakes to occur on the South American subduction zone. Rupture dimensions and distributions of slip on the plate interface differ in space and in time. For example, the 2001 Peru earthquake ruptured a smaller area of the interface than the 1868 earthquake which occurred in the same general area. Our PTHA methodology assumes that this variability can be approximately represented by a set of modelled scenarios for which the key parameters for impact at great distances from the source are the source location (specifically the midpoint of the rupture zone), and the seismic moment (TITOV *et al.*, 2001).

We establish a range of source locations (32 equally spaced source locations along the length of the Peru-Chilean subduction zone) – and seismic moments (corresponding to M_w 8.5 to 9.5 in increments of 0.1 magnitude units) that encompass the set of possible tsunamigenic earthquakes affecting New Zealand. For each combination of location and magnitude we estimate a credible slip distribution and surface deformation using appropriate scaling relationships (Fig. 2). This deformation is used as the initial input to a trans-Pacific tsunami propagation model and nested-grid model of impact on New Zealand. The estimates of maximum wave-heights from this set of model calculations, combined with a statistical model of the occurrence of each of the different source events, is then used to create a synthetic catalogue of source events and subsequent impacts on New Zealand using the Monte-Carlo technique (Fig. 3). This synthetic catalogue is generated in such a way that the modelled events have the same statistical properties as those estimated for the real events over an appropriately long time-scale. The synthetic catalogue of

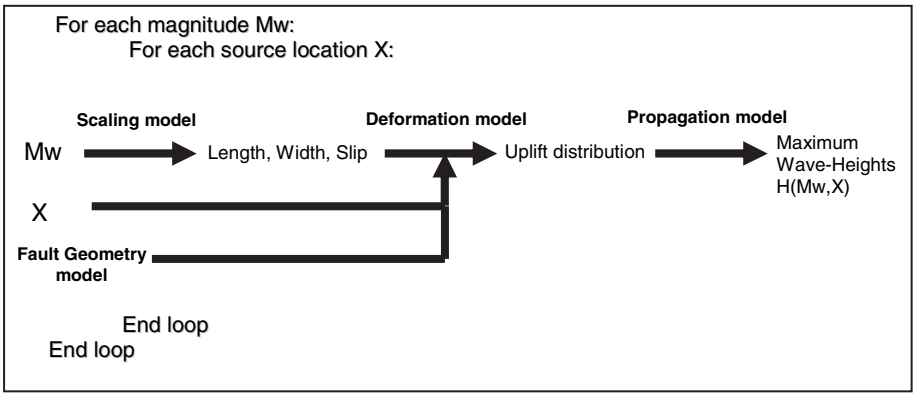

Figure 2
Outline procedure for estimating maximum wave heights for each combination of source location and moment magnitude. The maximum wave heights are stored for every point on the New Zealand nested grid.

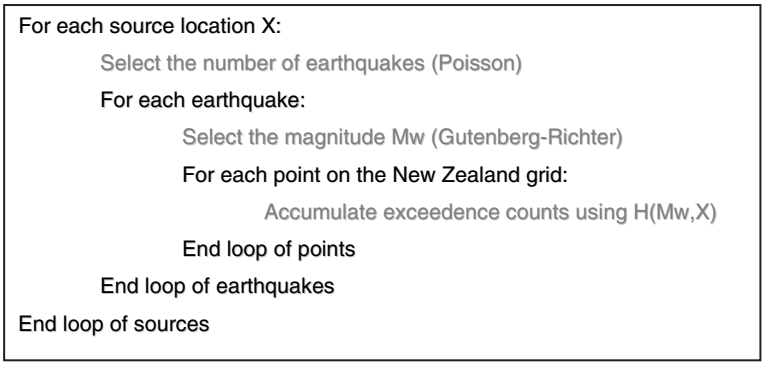

Figure 3
Outline Monte-Carlo procedure for generating synthetic catalogue of tsunami-generating events and subsequent impacts around New Zealand.

sources and impacts can then be used to estimate the hazard for any location of interest around the New Zealand coastline.

The procedure we have developed for PTHA requires the combination of several distinct models, each of which is described below.

Fault Geometry Model

The trough or trench was manually digitised with the assistance of the Integrated Tsunami Database software (ITDB/PAC, 2004). This is taken to represent the approximate up-dip extent of the plate interface at 2 km depth as shown in Figure 4. Based on analysis of deformation following the 1960 Chile earthquake BARRIENTOS and WARD (1990) have derived estimates of the cross section of the fault plane. Their modelling suggests an average dip on the fault plane of 20°, and an average width of 130 km, over the area of the 1960 rupture. As a first approximation for the purpose of developing the methodology, we have assumed that this cross section can be extended, at least approximately, along the full length of the subduction zone.

Scaling Model

The range of source magnitudes covered by this study initially ran from M_W 8.0 to 9.5. To estimate the deformation and fault length over this magnitude range, two different scaling models (Fig. 5) were used. From M_W 8.0 to 8.5 the relations of ABE (1975) were used to estimate typical rupture length, width and displacement for these magnitudes. Above magnitude 8.6 the rupture width extends for the full width of the fault plane (to the brittle-ductile boundary where fault locking no longer occurs). For these magnitudes we assume that the displacement continues to scale proportionately with the fault length; this is known as the L-model (SCHOLZ, 1982; HANKS and BAKUN, 2002). We found this model to give a better match to historical events on the

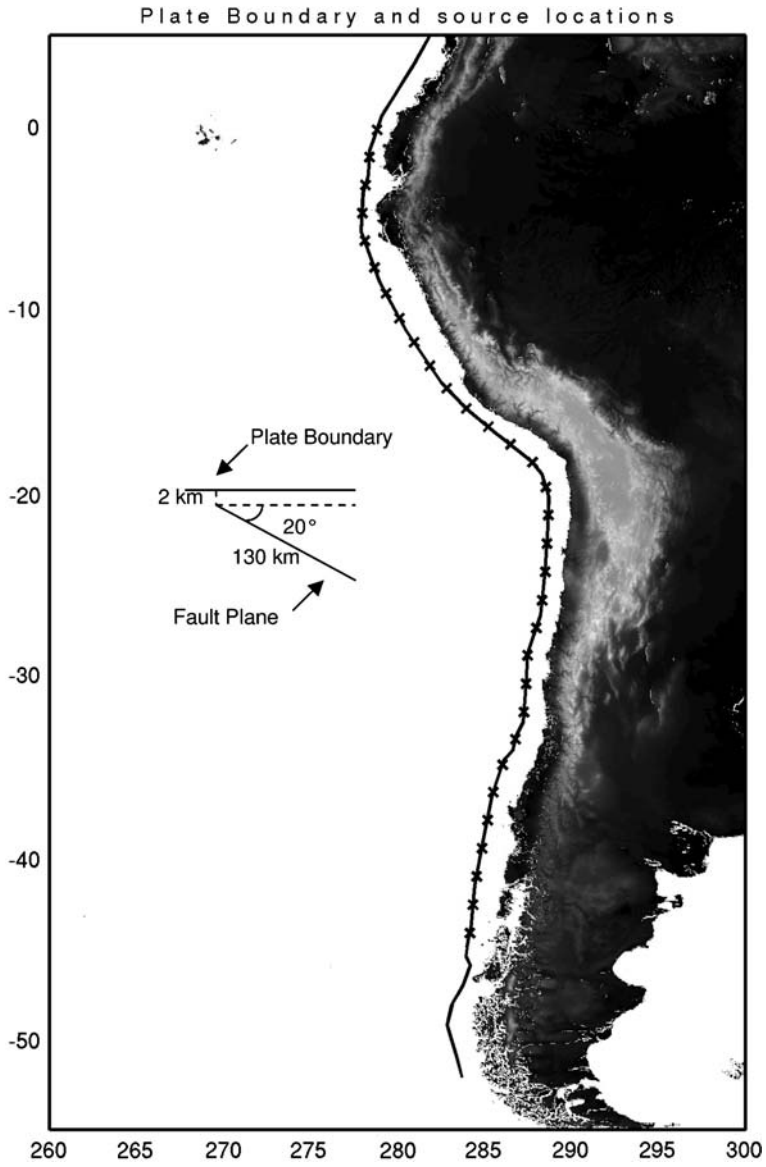

Figure 4
Digitised fault trace and assumed cross section for the plate interface. The crosses show the 32 source locations.

South American plate interface than the alternative W-model (ROMANOWICZ, 1992, 1994).

After initial trials, it was found that in general only earthquakes larger than about 8.5 were sufficient to produce tsunamis that were likely to cause damage in

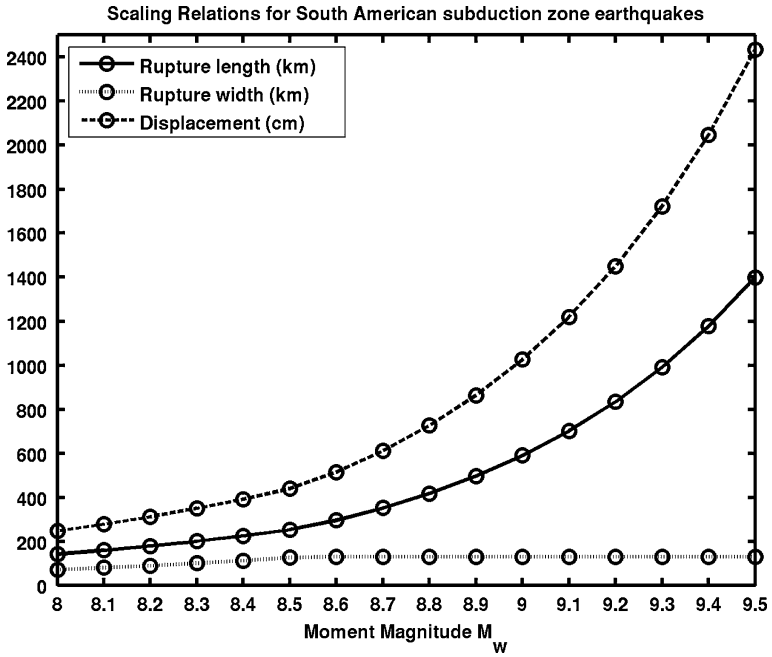

Figure 5
Scaling relations for rupture parameters as a function of moment magnitude.

New Zealand[1]. This is consistent with the historical record. Subsequently only sources in the range from 8.5 to 9.5 were included in our hazard calculations presented here.

Deformation Model

The deformation model is based on Okada's formula for deformation of an elastic half space (OKADA, 1985). Given the source location, rupture dimensions and geometrical model of the fault plane, a series of rectangular fault segments is calculated that collectively represent the rupture surface. It is assumed that the displacement is uniform over this compound surface. On each segment of the rupture surface it is assumed that the rupture is described by a pure 'thrust' mechanism with none of the moment taken up in strike-slip movement (for a discussion of slip-partitioning see MCCAFFREY, 1992, 1996).

[1] There remains the possibility that 'tsunami-earthquakes' (first recognised by KANAMORI, 1972) of magnitude less than M 8.5 could cause damaging tsunami in New Zealand, but these are not considered in this study. Some apparent 'tsunami earthquakes' may be due to underestimation of the true moment.

Propagation Model

The propagation of the tsunami, from its initiation by the deformation model uplift to its impact at the New Zealand shoreline, is calculated by using the MOST tsunami model (TITOV and GONZALEZ, 1997). Two modelling grids were used: The first covering the entire southern Pacific from 160°E–300°E and 65°S–5°N at a resolution of four minutes, and a one-minute nested grid allowing finer scale modelling of the tsunami at the New Zealand coastline.

The Pacific scale grid is based upon the one minute grid developed by Smith which blends the SMITH and SANDWELL (1997) gravity-derived dataset (accurate in deeper waters) with the GEBCO bathymetry database (more accurate in shallower waters). Around the New Zealand landmass the NZ National Institute for Water and Atmospheric Research contributed bathymetry data to the GEBCO dataset.

The finer nested grid, at one minute resolution, was derived by blending Smith's one-minute grid described above, with data gridded from C-MAP digital bathymetry supplied by Seabed Mapping of Nelson. This later dataset provides good resolution at shallow depths, particularly in the vicinity of ports and harbours. The one-minute nested grid covers the range from 165.6°E–179.5°E and 48.5°S–33.5°S.

The model treats the 10 m water depth contour as a reflecting boundary condition. The addition of finer grids and inundation calculations will be a future extension to this work. An empirical run-up factor can be used to relate the peak wave height at the 10 m contour to the on-land run-up height (see Results section).

Statistical Model

The statistical model describes the magnitude-frequency relationship for each source location. In this model the magnitude-frequency relationship is assumed to follow a truncated Gutenberg-Richter relationship with parameters a and b and maximum magnitude $M_{\max}$.

$$\begin{aligned} \frac{dN}{dM_W} &= 10^{a-bM_w} \qquad M_W < M_{\max} \\ &= 0 \qquad\qquad M_W \geq M_{\max} \end{aligned}$$

$$N(M > M_W) = \frac{10^a}{b\ln(10)}\left(10^{-bM_W} - 10^{-bM_{\max}}\right).$$

The values for these parameters are based upon those used by BERRYMAN (2005). Following this reference a b-value of 1 is assumed (Fig. 6)[2], as is a maximum

[2] Figure 6 is notable for the extent to which the global average b-value of 1 (WESNOUSKY, 1999) appears to hold even for the largest magnitude earthquakes; however some caution needs to be exercised as the sample size is small (8 events greater than magnitude 8.5 over 200 years).

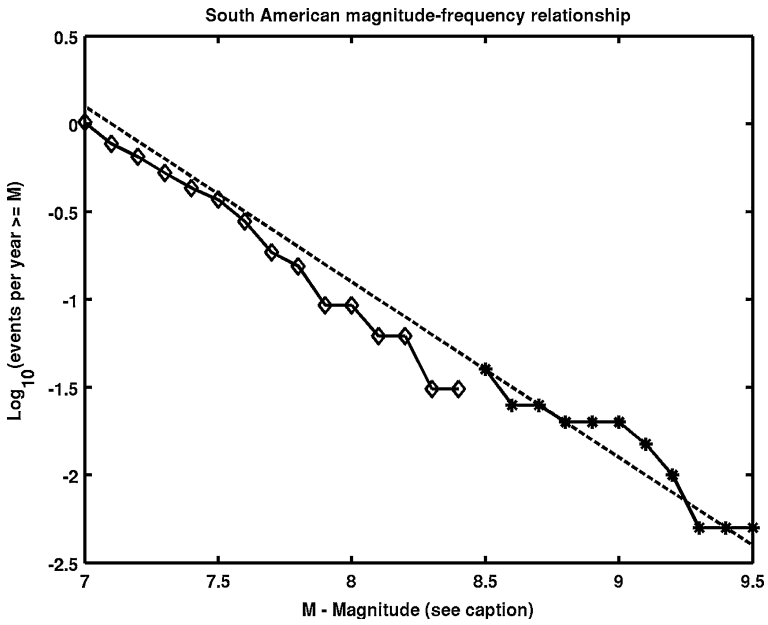

Figure 6

Magnitude-frequency relationship for the west coast of South America between 45°S and the equator. The data used to plot the diamonds are taken from the USGS/NEIC catalogue and spans from 1973 to May 2005. The data used to plot the asterisks are taken from the ITDB/PAC (2004) catalogue of tsunamigenic earthquakes (years 1803 to 2003, magnitudes ≥ 8.5), and the magnitude used is the first quoted value in the sequence: M_w, M_t, M_s. The two datasets are plotted as independent cumulative distributions. The dashed line represents a Gutenberg-Richter magnitude-frequency relationship with *b*-value of 1 and a recurrence interval of 25 years for $M \geq 8.5$, corresponding to 75% of the relative plate motion being released seismically.

magnitude of 9.5, corresponding to the upper limit of estimates of the moment of the 1960 Chile earthquake. This maximum magnitude is taken to apply throughout the length of the plate boundary. The *a*-values have been estimated assuming that 75% of the relative plate motion (perpendicular to strike) is released seismically on the plate interface. For this purpose the plate boundary has been divided into two types; between 19°S and 9°S where convergence is oblique, and the remaining locations where convergence is approximately orthogonal to the strike.

For the purpose of the Monte-Carlo method it is convenient to convert the *a*-values into recurrence intervals for earthquakes exceeding the threshold $M_{\min} = 8.5$. This leads to recurrence intervals of 9*110 = 990 years for the 9 source locations between 19°S and 9°S, and 23*32 = 736 years for the remaining 23 source locations. For the South American subduction zone as a whole the recurrence interval for exceeding $M_{\min}$ is then $1/(110^{-1} + 32^{-1}) \approx 25$ years (see comparison with the historical record in Fig. 6).

Monte-Carlo Generation of Synthetic Catalogue

The procedure for generating the synthetic catalogue of earthquake sources and tsunami impacts is outlined in Figure 3.

First a time span is chosen for the synthetic catalogue; this needs to be significantly longer than any of the time scales in the magnitude-frequency statistics to ensure that all possible events are sampled several times. Here we have used 500,000 years. For each source we then calculate the number of earthquakes exceeding $M_{\min}$ by sampling from a Poisson distribution, and for each of these earthquakes we calculate a magnitude by sampling from a truncated Gutenberg-Richter distribution. In this way the synthetic catalogue of sources is developed.

For the purpose of estimating tsunami hazard it is necessary to count the number of occasions when a given wave height is exceeded. This is done by incrementing an array of exceedence-counts, defined at all locations in the nested grid, after each event in the catalogue using the pre-calculated arrays $H(M_w, X)$. As our measure of hazard we use the double-amplitude H2, in this case estimated by doubling the maximum wave elevation over the ambient sea-level. The result is a count of the number of times that H2 exceeded 1 m, 2 m,..., 20 m at each point around the New Zealand coastline greater than 10 m deep over the period of the synthetic catalogue. From this information we can estimate the recurrence time for a given H2, and convert this information into a plot of H2 for a given return period using conventional PSHA techniques.

Results

The results shown below represent the tsunami hazard due to only one type of source, namely South American subduction zone earthquakes. The parameterisation of our model is preliminary and is used to illustrate the Monte-Carlo technique; future refinements are discussed in the following section.

In order to make the results more clearly visible on the printed page we have applied a technique described in Appendix 2.

The reason for plotting the tsunami double amplitude is to enable a link to the tsunami run-up height. KAJIURA (1983, 1986) showed that the double amplitude as measured from peak to trough by a tide gauge was a good estimate of the median run-up height measured in the vicinity of the tide gauge[3]. This is equivalent to assuming a run-up factor of 2 (see GEIST, 1998 and SATAKE, 1994 for discussion of run-up factors).

[3] However, some of this apparent amplification may be due to underestimation of the true waveheight due to filtering of the signal by the tide-gauge (SATAKE *et al.*, 1988). The association of modelled H2 with run-up should be regarded as tentative pending further calibration or more detailed modelling.

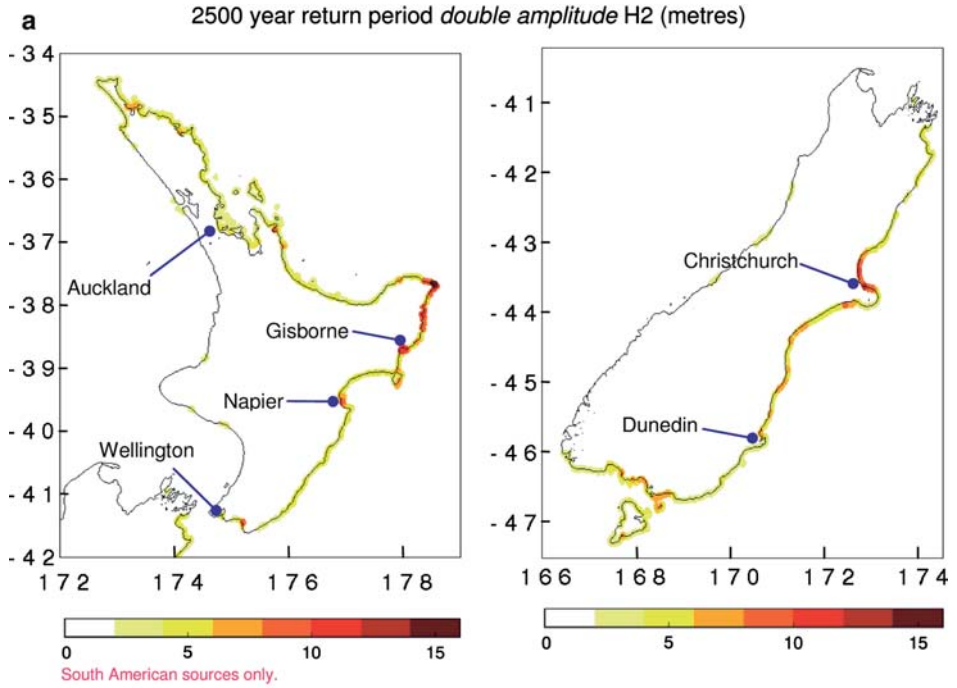
a
2500 year return period *double amplitude* H2 (metres)
Auckland
Gisborne
Napier
Wellington
Christchurch
Dunedin
South American sources only.

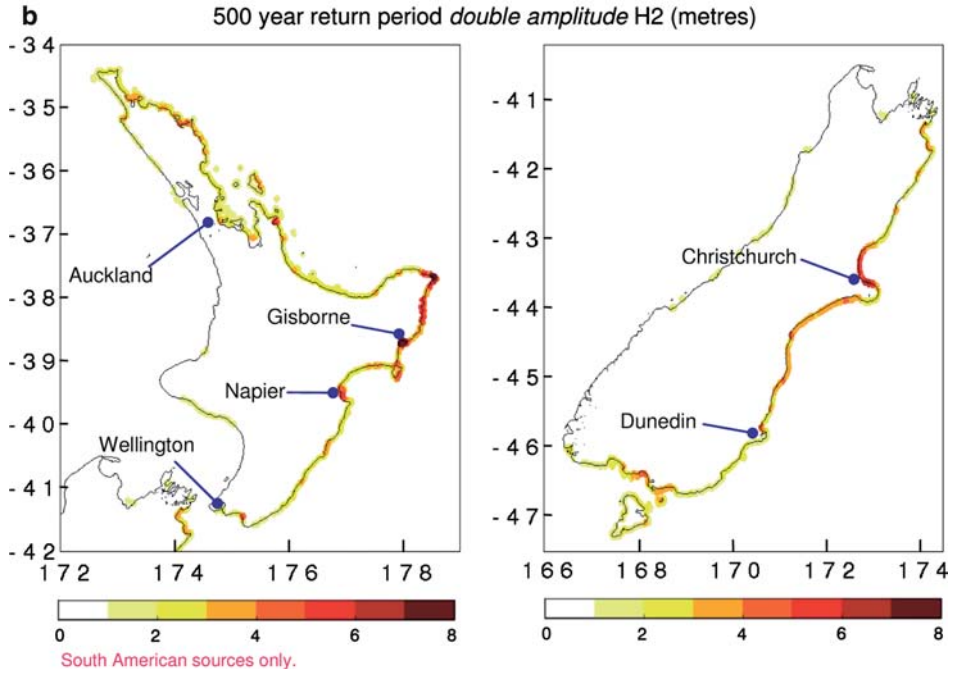
b
500 year return period *double amplitude* H2 (metres)
Auckland
Gisborne
Napier
Wellington
Christchurch
Dunedin
South American sources only.

◀

Figure 7
a. Double amplitude H2 in metres for the 2500-year return period South American tsunami at each location around the New Zealand coastline. H2 can be used as a first estimate of the median run-up within the surrounding area. **b.** Double amplitude H2 in metres for the 500-year return period South American tsunami at each location around the New Zealand coastline. H2 can be used as a first estimate of the median run-up within the surrounding area.

The results in Figures 7a and 7b show the values of H2 estimated for return periods of 2500 and 500 years, respectively. The general pattern of hazard is similarly distributed in both cases, and largely matches expectations based on the historical records of the 1868, 1877 and 1960 tsunamis. In particular we see high hazard around Banks Peninsula (immediately south of Christchurch) due to the wave-guiding effect of the Chatham rise (which extends east from Banks Peninsula to the Chatham Islands), and along the coast north of Gisborne, as has been observed historically. The hazard on Banks Peninsula appears historically to vary significantly from bay to bay, probably due to local resonances, an effect which is not apparent in our model due to the limited resolution of our nested grid. The elevated hazard level around the southern part of the South Island was not anticipated, and some important future work will be to disaggregate the hazard here to identify which sources are contributing.

Limitations and Future Refinements

We expect to make further refinements to the statistical and physical models of the earthquake sources. Our statistical model is relatively simple and based on the assumption that the plate-boundary is seismically homogeneous (except for the change in recurrence interval between 19°S and 9°S due to oblique convergence). A detailed study of the seismic characteristics of different sections of the plate-boundary will be a necessary step in the refinement of our model.

Our physical model of the sources assumes a uniform displacement over the rupture surface. It is known that slip distribution plays a significant role in the near-field (GEIST, 1998), and the far-field sensitivity to slip distribution is an area for future study.

The method shown here can be extended to include further levels of nested grid, and to include inundation modelling of specific key sites.

The addition of tides to the Monte-Carlo model is expected to be relatively straightforward in the first approximation: At any particular site the effect of tides on the median run-up height (estimated by H2) can be modelled by randomly sampling for the phase of the tide at which the peak wave arrives. It should be noted that for distant-source tsunami the time-envelope of the arriving wave-train may stretch over several wave-periods; in this case the highest combination of wave and tide may not

necessarily occur at the moment of the peak wave, and more careful modelling is required.

Most practical uses of PTHA will require the inclusion of all hazardous tsunami sources affecting New Zealand, in particular earthquakes on the plate boundary which pass through New Zealand.

Conclusions

We conclude that a PTHA for distant source tsunami is feasible, using techniques similar to those used for PSHA. The Monte-Carlo approach presented here is relatively simple to use, though moderately demanding of computer time. The model we present produces results consistent with the historical record of South American tsunamis, and should be extended to include all known tsunami sources likely to be hazardous in New Zealand.

Acknowledgements

We gratefully acknowledge the assistance of: Warwick Smith, Phil Scadden and John Beavan at GNS Science; Vasily Titov, Harold Mofjeld and Frank Gonzalez at NOAA PMEL; and Jose Borrero at ASR Limited.

Appendix 1 Major Historical Trans-Pacific Tsunami

1868

In 1868 a great earthquake of magnitude 9.1 (ITDB/PAC, 2004) occurred along the southern coastline of Peru and northernmost area of Chile. The rupture area is estimated to have extended for at least 500 km northwest from Arica in Chile (COMTE and PARDO, 1991), although recent results suggest it may have extended significantly further than this (OKAL *et al.*, 2006). Locally run-ups of 15 m were reached (ITDB/PAC, 2004).

Numerical modelling developed for this paper shows that tsunami sourced from plate interface events in this region are orientated in such a way that a large proportion of the wave energy is directed towards New Zealand. Unsurprisingly then, the impact of this tsunami on New Zealand was significant, though somewhat lessened by the good fortune of arriving near low-tide in many parts of the country.

Maximum run-ups on the East Coast were widely distributed in the range between 1 and 2 metres, but were significantly higher in a number of specific locations, notably Banks Peninsula (3–4 m), the Canterbury coast (4 m), the Bay of

Plenty (3 m) and the Chatham Islands (10 m) (Downes, unpublished New Zealand Tsunami Database).

1877

The 1877 great earthquake in northern Chile is estimated to have had a magnitude of approximately 8.8, and to have ruptured along a length of about 400 km extending south from Arica (the southernmost limit of the 1868 rupture zone) (COMTE and PARDO, 1991). Local run-up heights for this event exceeded 20 metres. This area of South American coastline is less effective at directing tsunami waves towards New Zealand. More energy was directed to the north with run-up heights of 4–5 m observed in Hawaii and Japan.

Around New Zealand run-up heights were again widely observed in the 1–2 m range, though typically lower than for the 1868 event at the same locations. The highest maximum wave height observations were in the 3–4 m range (Downes, unpublished New Zealand Tsunami Database).

1960

The magnitude 9.5 Chile earthquake of 1960 (KANAMORI and ANDERSON, 1975) is well-known for being the largest earthquake to be instrumentally recorded (OKAL and TALANDIER, 1991). The rupture zone extended for approximately 1000 km south from the Arauco Peninsula (CIFUENTES, 1989). The subsequent tsunami caused great damage locally, with peak run-up heights of about 25 metres. The orientation of the rupture zone directed the tsunami energy towards the north, and large run-up heights were recorded in Hawaii (up to 12 m) and Japan (up to 6.4 m); severe damage and loss of life occurred in these locations.

Many locations on the New Zealand east coast observed peak run-up heights in the range from 0.5 to 1.5 m. Largest observations were in Gisborne and Napier (4–5 m), and around Banks Peninsula (3–4 m). As in 1868, the impact was reduced by the largest waves occurring near low tide over a significant part of the coast (Downes, unpublished New Zealand Tsunami Database).

Appendix 2 Processing of Results for Representation on a Small Map

When a one minute grid is used for estimating tsunami hazard we encounter the problem that the hazard values (in our case H2 wave heights) at points closest to the coast form a strip which is too small to see clearly on the printed page. To resolve this issue we apply the following procedure:

All points within a 3.5-grid cell distance of the 10 m isobath are selected. For each of these points the colour used to represent the wave height is chosen based on the highest wave height at any point within a 3.5-grid cell radius.

This process therefore emphasises the largest hazard within the vicinity of a particular location. Although this procedure is principally intended to improve legibility, it also represents a conservative assumption regarding the uncertainties in propagating from the 10 m isobath to the shoreline.

References

Abe, K. (1975), *Reliable estimation of the seismic moment of large earthquakes*, J. Phys. Earth. *23*, 381–390.

Annaka, T., Satake, K., Shuto, N., Sakayima, T., and Yanagisawa, K. (2004), *Logic-tree approach for Probabilistic Tsunami Hazard Analysis and its applications to the Japanese Coasts*, Eos Trans. AGU, 85(47), Fall Meet. Suppl., Abstract OS23D-1349.

Barrientos, S.E. and Ward, S.N. (1990), *The 1960 Chile earthquake; inversion for slip distribution from surface deformation*, Geophys. J. Internat. *103*(3), 589–598.

Ben-Menahem, A. and Rosenman, M. (1972), *Amplitude patterns of tsunami waves from submarine earthquakes,* J. Geophys. Res. *77*, 3097–3128.

Berryman, K. (compiler) (2005), *Review of tsunami hazard and risk in New Zealand*, Institute of Geological and Nuclear Sciences client report 2005/104. http://www.civildefence.govt.nz/memwebsite.nsf/wpg_URL/For-the-CDEM-Sector-Publications-Tsunami-Risk-and-Preparedness-in-New-Zealand?OpenDocument.

Borrero, J.C. (2005), *Field survey of Northern Sumatra and Banda Aceh, Indonesia after the Tsunami and earthquake of 26 December 2004*, Seismol. Res. Lett. *76*(3), 312–320.

Cifuentes, I.L. and Silver, P.G. (1989), *Low-frequency source characteristics of the great 1960 Chilean earthquake*, J. Geophys. Res. *94*(B1), 643–663.

Cochran, U.A., Berryman, K.R., Mildenhall, D.C., Hayward, B.W., Southall, K., and Hollis, C.J. (2005), *Towards a record of Holocene tsunami and storms for Northern Hawke's Bay, New Zealand.* New Zealand J. Geol. Geophys. *48*, 507–515.

Comte, D. and Pardo, M. (1991), *Reappraisal of great historical earthquakes in the northern Chile and southern Peru seismic gaps*, Natural Hazards *4*, 23–44.

Cornell, C.A. (1968), *Engineering seismic risk analysis*, Bull. Seismol. Soc. Am. *58*(5), 1583–1606.

Ghobarah, A., Saatcioglu, M., and Nistor, I. (2006), *The impact of the 26 December 2004 earthquake and tsunami on structures and infrastructure,* Eng. Struct. *28*(2), 312–326.

Geist, E.L. (1998), *Local tsunamis and earthquake source parameters*, Advan. Geophys. *39*, 117–209.

Goff, J.R., Rouse, H.L., Jones, S.L., Hayward, B.W., Cochran, U., McLea, W., Dickinson, W.W., and Morley, M.S. (2000), *Evidence for an earthquake and tsunami about 3100–3400 yrs. ago, and other catastrophic saltwater inundations recorded in a coastal lagoon, New Zealand,* Marine Geology *170*, 231–249.

Hanks, T.C. and Bakun, W.H. (2002), *A bilinear source-scaling model for M-log A observations of continental earthquakes*, Bull. Seismol. Soc. Am. *92*(5), 1841–1846, illus. incl. 1 table, 28 refs.

Iida, K., Cox, D. and Pararas-Carayannis, G. (1967), *Preliminary Catalogue of Tsunamis occurring in the Pacific Ocean*, Data Report N 5, HIG 67-10, Hawaiian Inst. of Geophysics, University of Hawaii, 274 p.

ITDB/PAC (2004), *Integrated Tsunami Database for the Pacific*, Version 5.1 of June 2004. CD-ROM, Tsunami Laboratory, ICDMMG SD RAS, Novosibirsk, Russia.

KAJIURA, K. (1983), *Some statistics related to observed tsunami heights along the coast of Japan*, In (K. Iida and T. Iwasaki, eds.), *Tsunamis – Their Science and Engineering* (Terra. Sci. Publ., Tokyo, 131–145.

KAJIURA, K. (1986), *Height distribution of the tsunami generated by the Nihonkai-Chubu (Japan Sea Central Region) Earthquake*, Science of Tsunami Hazards *4*(1), 3–14.

KANAMORI, H. (1972), *Mechanism of tsunami earthquakes*, Phys. Earth Planet. and Inter. *6*, 346–359.

KANAMORI, H. and ANDERSON, D.L. (1975), *Amplitude of the Earth's free oscillations, and long-period characteristics of the earthquake source*, J. Geophys. Res. *80*, 1075–1078.

LOCKRIDGE P.A. (1985), *Tsunamis in Peru-Chile*, Report SE-39, Boulder, WDC-A for Solid Earth Geophysics, 97 p.

MCCAFFREY, R. (1992), *Oblique plate convergence, slip vectors, and forearc deformation*, J. Geophys. Res. *97*, B6, 8905–8915.

MCCAFFREY, R. (1996), *Estimates of modern arc-parallel strain rates in fore arcs*, Geology *24*(1), 27–30.

MCGUIRE, R. (2004), *Seismic hazard and risk analysis*, MNO-10 (Earthquake Engineering Research Institute, USA).

MUSSON, R.M.W. (2000), The use of Monte Carlo simulations for seismic hazard assessment in the U.K., Annali di Geofisica *43*(1), 1–9.

NICHOL, S.L., LIAN, O.B., and CARTER, C.H. (2003), *Sheet-gravel evidence for a late Holocene tsunami run-up on beach dunes, Great Barrier Island*, New Zealand, Sediment. Geol. *155*, 129–145.

OKADA, Y. (1985), *Surface deformation due to shear and tensile faults in a half-space*, Bull. Seismol. Soc. Am. *75*(4), 1135–1154.

OKAL, E.A., SYNOLAKIS, C.E., FRYER, G.J., HEINRICH, P., BORRERO, J.C., RUSCHER, C., ARCAS, D., GUILLE, G. and ROUSSEAU, D. (2002), *A field survey of the 1946 Aleutian tsunami in the far field*, Seismol. Res. Lett. *73*, 490–503.

OKAL, E.A., BORRERO, J.C. and SYNOLAKIS, C.E. (2006), *Evaluation of tsunami risk from regional earthquakes at Pisco, Peru*, Bull. Seismol. Soc. Am. (in press).

OKAL, E.A. (2003), *Normal mode energetics for far-field tsunamis generated by dislocations and landslides*, Pure Appl. Geophys. *160*, 2189–2221.

OKAL, E.A. and TALANDIER, J. (1991), *Single-station estimates of the seismic moment of the 1960 Chilean and 1964 Alaskan earthquakes, using the mantle magnitude* M_{m}, Pure Appl. Geophys. *136*, 103–126.

POWER, W., DOWNES, G., MCSAVENEY, M., BEAVAN, J., and HANCOX, G. (2005), *The Fiordland earthquake and tsunami, New Zealand, 21 August 2003*. In *Tsunamis: Case Studies and Recent Developments*, vol. 23 of the series *Advances in Natural and Technological Hazards Research*, (Springer, New York, VIII).

RIKITAKE, T. and AIDA, I. (1988), *Tsunami hazard probability in Japan*, Bull. Seismol. Soc. Am. *78*(3), 1268–1278.

ROMANOWICZ, B. (1992), *Strike-slip earthquakes on quasi-vertical transcurrent faults: Inferences for general scaling relations*, Geophys. Res. Lett. *19*, 481–484.

ROMANOWICZ, B. (1994), *Comment on 'A reappraisal of large earthquake scaling' by C. Scholz*, Bull. Seismol. Soc. Am. *84*, 1675–1676.

SATAKE, K., OKADA, M., and ABE, K. (1988), *Tide gauge response to tsunamis: Measurements at 40 tide gauge stations in Japan*, J. Marine Res. *46*, 557–571.

SATAKE, K. (1994), *Mechanism of the 1992 Nicaragua tsunami earthquake*, Geophys. Res. Lett. *21*, 2519–2522.

SCHOLZ, C.H. (1982), *Scaling laws for large earthquakes; consequences for physical models*, Bull. Seismol. Soc. Am. *72*(1), 1–14.

SMITH, W.H.F. and SANDWELL, D.T. (1997), *Global sea floor topography from satellite altimetry and ship depth soundings*, Science *277*(5334), 1956–1962.

THIO, H.K., I., G. and SOMMERVILLE, P. (2005), *Probabilistic tsunami hazard analysis,* IASPEI General Assembly, Abstract 636.

TITOV, V.V. and GONZALEZ, F.I. (1997), *Implemenation and testing of the method of splitting tsunami (MOST) model,* NOAA Technical Memorandum ERL PMEL-112.

TITOV, V.V., MOFJELD, H.O., GONZÁLEZ, F.I., and NEWMAN, J.C. (2001), *Offshore forecasting of Alaskan tsunamis in Hawaii*, In (G.T. Hebenstreit, ed.), *Tsunami Research at the End of a Critical Decade* (Kluwer, Netherlands, pp.75–90).

TITOV, V.V., RABINOVICH, A.B., MOFJELD, H.O., THOMSON, R.E., and GONZÁLEZ, F.I. (2005), *The global reach of the 26 December 2004 Sumatra tsunami*, Science *209*, 2045–2048.

WATTS, P. (2004), *Probabilistic predictions of landslide tsunamis off Southern California*, Marine Geology *203*, 281–301.

(Received February 5, 2006, accepted June 26, 2006)
Publised Online First: January 30, 2007